Supplementary Information

1. Reagent

Copper chloride dihydrate (≥99%, Sigma-Aldrich), dicyandiamide (99%, Sigma-Aldrich), benzyl alcohol (99.5%, ChemPure), benzaldehyde (≥99.5%, ChemPure), potassium iodide (≥99.5%, ChemPure), potassium hydrogen phthalate (>99.8%, ChemSolute), 5,5-dimethyl-1-pyrroline N-oxide, DMPO (≥99%, Sigma-Aldrich), 2,2,6,6-tetramethylpiperidine- 1-oxyl, TEMPO (99%, Sigma-Aldrich), 2,2,6,6-Tetramethylpiperidine, TEMP (≥99%, Sigma-Aldrich), 1,4-benzoquinone (≥98%, Sigma-Aldrich), silver nitrate (99.8%, Stanlab), *tert*-Butanol (≥99%, Carl Roth), Cu_2O (99.5%, FUJIFILM Wako), and CuO (99.9%, FUJIFILM Wako) were used as received. Ultrapure water the Milli-Q® system was used throughout all the experiments.

2. Determination of Photocatalytic Performance

The photocatalytic performance, i.e., BA conversion, BAL yield, and BAL selectivity, was calculated using the following equations.

$$Conversion\ (\%) = \left(\frac{C_0 - C_r}{C_0}\right) \times 100 \qquad (1)$$

$$Yield\ (\%) = \left(\frac{C_p}{C_0}\right) \times 100 \qquad (2)$$

$$Selectivity\ (\%) = \left(\frac{C_p}{C_0 - C_r}\right) \times 100 \qquad (3)$$

$$Aromatic\ balance\ (\%) = \left(\frac{C_r + C_p}{C_0}\right) \times 100 \qquad (4)$$

where C_0 is the initial BA concentration (mmol L^{-1}). C_r and C_p are the concentration of reactant (BA) and product (BAL) when sampling, respectively.

3. Determination of Apparent Quantum Yield

The apparent quantum yield (AQY) was calculated using the following equation.

$$AQY\ (\%) = \left(\frac{2vN_A hc}{IA\lambda}\right) \times 100 \qquad (5)$$

where v is the rate of BAL production (mol s^{-1}), N_A is the Avogadro's number (6.02×10^{23} mol^{-1}), h is Planck's constant (6.62×10^{-34} J s), c is the speed of light (3.0×10^{8} m s^{-1}), I is the light intensity (1513 W m^{-2}), A is the irradiation area (1.25×10^{-5} m^2), and λ is the light wavelength (455 nm).

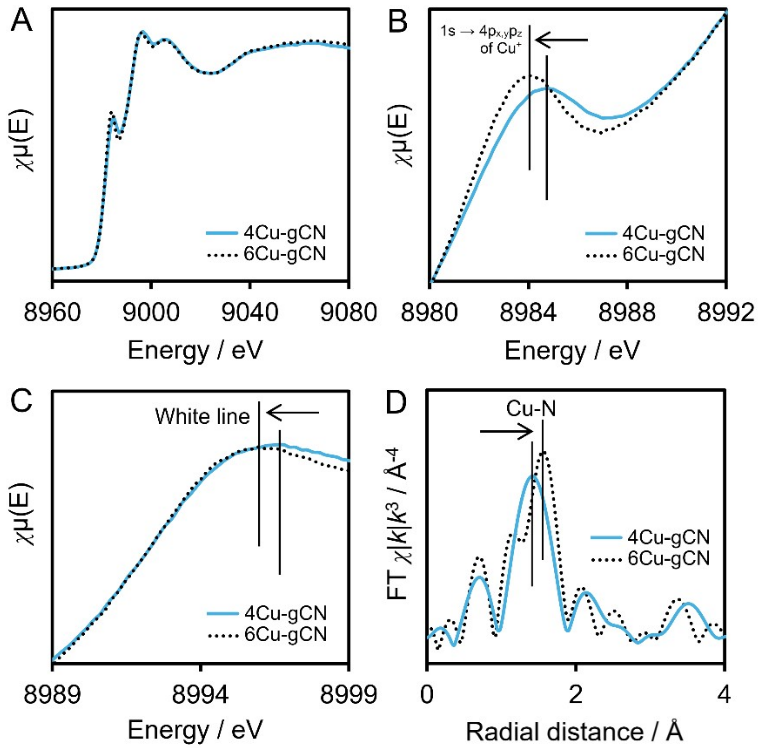

Figure S1. XANES spectra showing (A) the overall features, (B) the feature corresponding to Cu 1s → 4p transitions, and (C) a weak feature just after the absorption edge (white line). (D) FT-EXAFS spectra for the Cu-N coordination in R space.

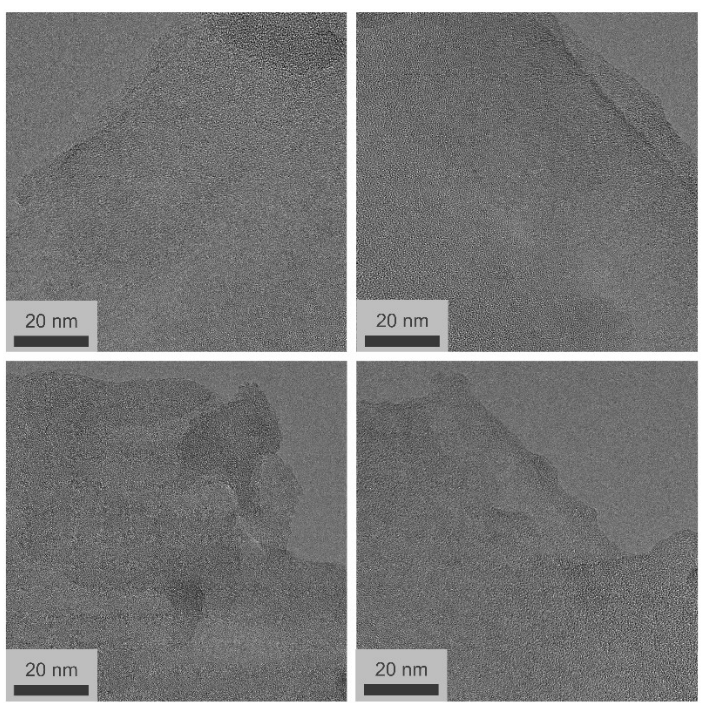

Figure S2. HR-TEM images of 4Cu-gCN taken from different regions of the sample.

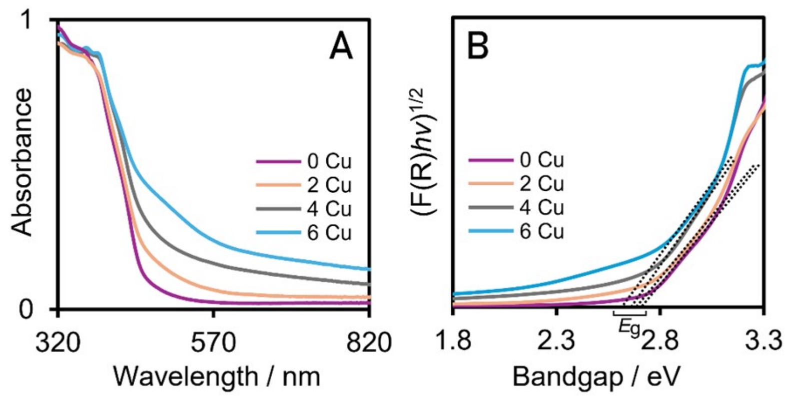

Figure S3. (A) DRS spectra and (B) Tauc's plots of the prepared samples.

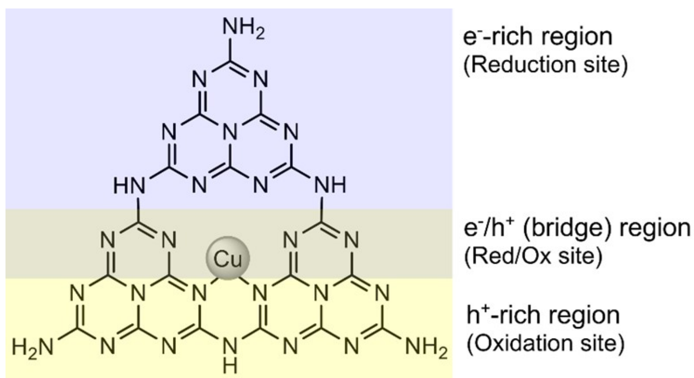

Figure S4. Schematic of spatially separated redox sites in the Cu-gCN cluster, enabling excited electrons to be spatially separated from holes, thereby retarding recombination.

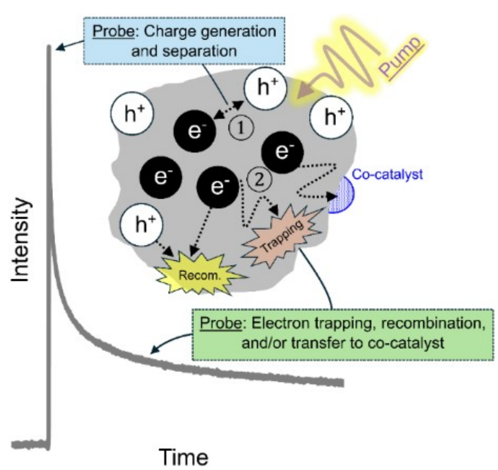

Figure S5. Schematic of the different photophysical phenomena that can be probed by TRMC.

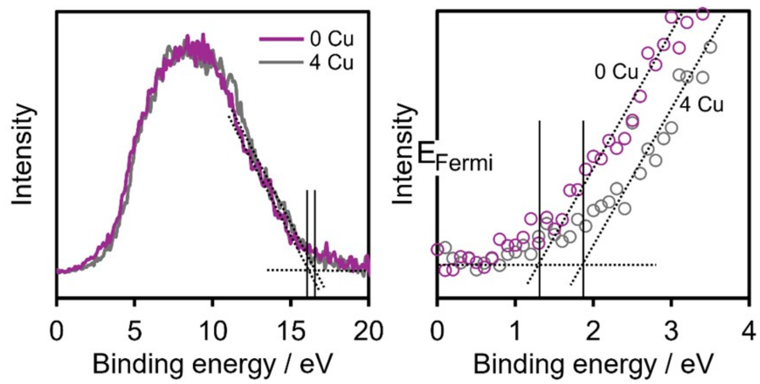

Figure S6. UPS spectra of gCN and 4Cu-gCN. The left figure shows photoelectron signal plotted with respect to the Fermi level at 0 eV and showing determination of the secondary electron cut-off (SECO). The right figure shows the region near the Fermi level, showing the determination of the VB edge.

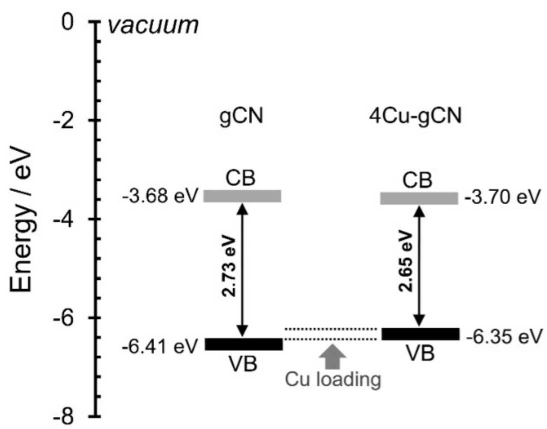

Figure S7. Band structures of gCN and 4Cu-gCN constructed based on UPS and DRS data.

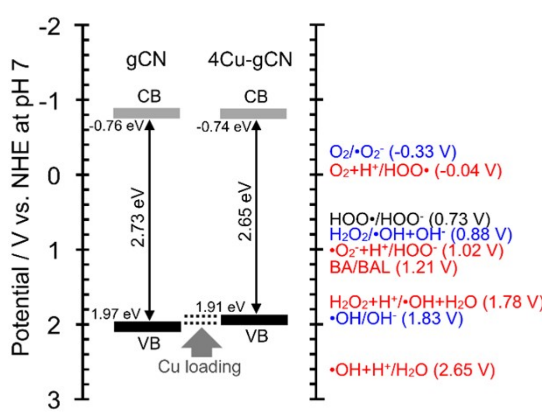

Figure S8. Band structures of gCN and 4Cu-gCN determined from UPS and DRS data. The standard redox potentials (E^0) are taken from Ref. [1-4]. Redox couples written in red, blue, and black indicate that the corresponding redox reactions tend to proceed at acidic, basic, and neutral conditions, respectively.

Table S1. Recycling tests for gCN and 4Cu-gCN.

Cu loading (wt.%)	BA conv. (%)	BAL yield (%)	BAL sel. (%)	Arom. Bal. (%)	AQY (%)	YPR (mmol g^{-1} h^{1} W^{-1})
0	56	18	32	64	0.16	0.20
	51	17	33	66	0.15	0.19
	53	15	28	62	0.13	0.17
	44	12	27	68	0.10	0.14
4	97	97	100	100	0.84	1.07
	92	92	100	100	0.79	1.02
	85	76	89	91	0.66	0.84
	87	82	94	95	0.71	0.91

Conditions: BA (1 mmol L^{-1}, 0.01 mmol), photocatalyst (0.5 g L^{-1}, 5 mg), time (4 h), and irradiance (0.45 W, 455 nm).

Table S2. Partial oxidation of BA over g-C_3N_4-based photocatalysts

Catalyst	Precursor[a]	S_{BET} (m^2 g^{-1})	Con. (g L^{-1})	Light source	*t* (h)	BA con. (mmol L^{-1})	BA conv. (%)	BAL sel. (%)[b]	YPR[c]	Ref.
P-gC_3N_4	Melamine	4	0.33	Fluorescent lamps (3 ×15 W, 340-420 nm)	4	500 (acetonitrile)	5	52	0.21	5
P-gC_3N_4	Urea	16					4	45	0.15	
P-gC_3N_4	Thiourea	28					3	36	0.09	
Pt@gC_3N_4	Melamine	6	0.625	Xe lamp (200 W, ≥420 nm,	5	10 (water)	27	90	<0.01	6
P/gC_3N_4	Urea	*n.a.*	2	LED lamp (64 W, 465 nm)	10	50 (acetonitrile, O_2)	96	>99	0.04	7
gC_3N_4	Melamine	*n.a.*	0.67	Fluorescent lamps (6 × 15 W, 315-400 nm)	4	0.5 (water)	29	88	<0.01	8
gC_3N_4	Cyanamide	130	2.5	Xe lamp (300 W, >420 nm)	3	40 (water, 0.8 MPa O_2)	10	96	<0.01	9
CdS/gC_3N_4	Melamine	7	6.67	Xe lamp (300 W, >420 nm)	4	25.5 (benzotrifluoride, 0.5 MPa N_2)	48	93	<0.01	10
S-gC_3N_4	Dicyandiamide	66	5	Xe lamp (300 W, >420 nm)	4	100 (trifluorotoluene, 0.1 MPa O_2)	19	>99	<0.01	11
gC_3N_4	Cyanamide	200	5	Xe lamp (300 W, >420 nm)	3	100 (acetonitrile, 0.8 MPa O_2)	70	68	0.01	12
NHPI/gC_3N_4*	Cyanamide	*n.a.*	10	W-filament bulb (250 W, >420 nm)	22	500 (toluene, 5 mL min^{-1} O_2)	89	94	<0.01	13
gC_3N_4	Melamine	*n.a.*	3.75	Hg lamp (100 W, >400 nm)	3	25 (water, O_2)	96	82	0.02	14
gC_3N_4	Melamine	43	1.67	LED lamps (18 × 1 W, 395 nm)	5	2 (acetonitrile)	77	87	<0.01	15
gC_3N_4	Urea	53					85	85	<0.01	
Fe@gC_3N_4	Melamine	*n.a.*	2.5	LED lamp (18 W, >400 nm)	3	200 (acetonitrile, 3 mL H_2O_2)	93	>99	1.36	16
MIL/Ag/gC_3N_4	Melamine	101	0.83	Xe lamp (500 W, >400 nm)	6	33.4 (water, O_2)	47	97	<0.01	17
TiO_2/gC_3N_4	Urea	68	2.5	Xe lamp (400 W, >400 nm)	4	100 (acetonitrile, O_2)	42	>99	0.01	18
Ru@B-gC_3N_4	Melamine	2.5	0.5	UVA lamp (2×18 W, 365 nm)	3	0.5 (water)	83	57	<0.01	19
Fe_2O_3/gC_3N_4	Melamine	27	1	Hg lamp (125 W, 365 nm)	4	100 (acetonitrile, 25 mL min^{-1} O_2)	20	34	0.01	20
ZnO/gC_3N_4	Melamine	10					9	26	<0.01	
S-gC_3N_4	Melamine	9	0.5	UVA lamps (9W, 365 nm)	5	0.5 (water)	22	63	<0.01	21
BiOBr/gC_3N_4	Melamine	11	0.4	Xe lamp (275 W, >400 nm)	5	0.1 (water)	95	18	<0.01	22
Cu-gC_3N_4	Dicyandiamide	13	0.5	LED lamp (0.45 W, 455 nm)	4	1 (water)	96	>99	1.07	This work

*N-hydroxyphthalimide (NHPI). [a]Precursor for the gC_3N_4. [b]Selectivity to BAL. [c]mmol BAL g^{-1} h^{-1} W^{-1}.

Table S3. Partial oxidation of BA in the presence of scavengers or additives.

Scavenger or additive	Scavenged species	Cu loading (wt.%)	BA conv. (%)	BAL yield (%)	BAL sel. (%)	Arom. Bal. (%)
None		0	53	19	36	66
		4	96	96	100	100
O_2		4	100	100	100	100
Ar		4	91	91	100	100
$AgNO_3$ (2 equiv.)	e^-	0	37	11	30	74
		4	88	87	99	99
KI (2 equiv.)	h^+	0	41	17	41	76
		4	54	47	87	93
BQ (1 equiv.)	$\bullet O_2^-$	0	32	13	40	81
		4	79	73	92	94
t-BuOH (1 equiv.)	•OH	0	51	13	25	62
		4	92	86	94	94
DMPO (2 equiv.)	•OH, $\bullet O_2^-$	0	28	11	39	83
		4	85	75	88	90
TEMP (2 equiv.)	$^1O_2$	0	50	16	32	66
		4	96	93	97	97
TEMPO (3 equiv.)	Organic radicals	0	48	24	50	76
		4	91	82	90	91

Conditions: BA (1 mmol L^{-1}, 0.01 mmol), photocatalyst (0.5 g L^{-1}, 5 mg), and reaction time (4 h).

Table S4. H_2O_2 production determined using the iodometric method.[23-25]

Cu loading (wt.%)	BAL yield (mmol L^{-1})	H_2O_2 yield (mmol L^{-1})
0	0.21	0.19
2	0.89	0.53
4	0.94	0.40
6	0.70	0.36
	Calibration curve	Results

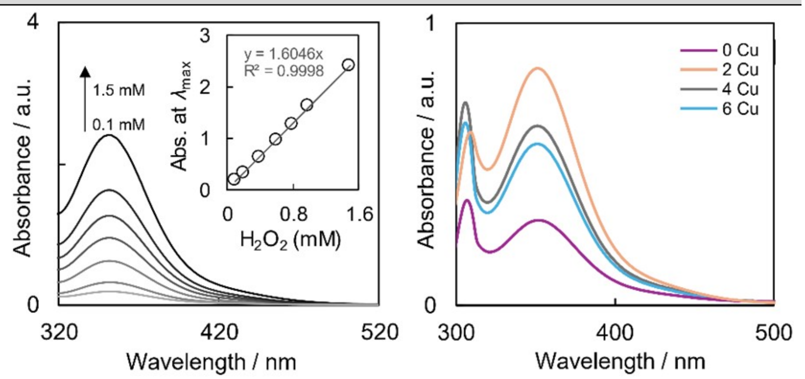

References

1. J. Choi, B. H. Suryanto, D. Wang, H.-L. Du, R. Y. Hodgetts, F. M. Ferrero Vallana, D. R. MacFarlane and A. N. Simonov, *Nature communications*, 2020, **11**, 5546.
2. G. Liao, C. Li, X. Li and B. Fang, *Cell Reports Physical Science*, 2021, **2**, 100355.
3. S. Wu and X. Quan, *ACS ES&T Engineering*, 2022, **2**, 1068-1079.
4. X. Xiao, J. Jiang and L. Zhang, *Applied Catalysis B: Environmental*, 2013, **142**, 487-493.
5. M. Bellardita, E. I. García-López, G. Marcì, I. Krivtsov, J. R. García and L. Palmisano, *Applied Catalysis B: Environmental*, 2018, **220**, 222-233.
6. T. Huo, Q. Deng, F. Yu, G. Wang, Y. Xia, H. Li and W. Hou, *ACS Applied Materials & Interfaces*, 2022, **14**, 13419-13430.
7. S. K. Pahari and R.-A. Doong, *ACS Sustainable Chemistry & Engineering*, 2020, **8**, 13342-13351.
8. I. Krivtsov, M. Ilkaeva, E. I. García-López, G. Marcì, L. Palmisano, E. Bartashevich, E. Grigoreva, K. Matveeva, E. Díaz and S. Ordóñez, *ChemCatChem*, 2019, **11**, 2713-2724.
9. B. Long, Z. Ding and X. Wang, *ChemSusChem*, 2013, **6**, 2074-2078.
10. X. Dai, M. Xie, S. Meng, X. Fu and S. Chen, *Applied Catalysis B: Environmental*, 2014, **158**, 382-390.
11. L. Zhang, D. Liu, J. Guan, X. Chen, X. Guo, F. Zhao, T. Hou and X. Mu, *Materials Research Bulletin*, 2014, **59**, 84-92.
12. F. Su, S. C. Mathew, G. Lipner, X. Fu, M. Antonietti, S. Blechert and X. Wang, *Journal of the American Chemical Society*, 2010, **132**, 16299-16301.
13. P. Zhang, J. Deng, J. Mao, H. Li and Y. Wang, *Chinese Journal of Catalysis*, 2015, **36**, 1580-1586.
14. V. Shvalagin, M. Kompanets, O. Kutsenko, S. Y. Kuchmy and M. Skoryk, *Theoretical and Experimental Chemistry*, 2020, **56**, 111-116.
15. R. Morozov, M. Golovin, D. Uchaev, A. Fakhrutdinov, M. Gavrilyak, I. Arkhipushkin, V. Boronin, V. Korshunov, F. Podgornov and I. Taydakov, *Journal of Chemical Sciences*, 2021, **133**, 1-17.
16. M. Devi, S. Ganguly, B. Bhuyan, S. S. Dhar and S. Vadivel, *European Journal of Inorganic Chemistry*, 2018, **2018**, 4819-4825.
17. Z. Yang, X. Xu, X. Liang, C. Lei, Y. Cui, W. Wu, Y. Yang, Z. Zhang and Z. Lei, *Applied catalysis B: environmental*, 2017, **205**, 42-54.
18. M. Mohammadi, H. Hadadzadeh, M. Kaikhosravi, H. Farrokhpour and J. Shakeri, *Molecular Catalysis*, 2020, **490**, 110927.
19. R. R. Solís, M. A. Quintana, G. Blázquez, M. Calero and M. J. Muñoz-Batista, *Catalysis Today*, 2023, **423**, 114266.
20. K. Cerdan, W. Ouyang, J. C. Colmenares, M. J. Munoz-Batista, R. Luque and A. M. Balu, *Chemical Engineering Science*, 2019, **194**, 78-84.
21. M. A. Quintana, R. R. Solís, G. Blázquez, M. Calero and M. J. Munoz-Batista, *Applied Surface Science*, 2024, **656**, 159717.
22. W. Wang, X. Cong, X. Zhang, W. Xu, J. Diao, Y. Bao and F. Guo, *Journal of Environmental Chemical Engineering*, 2025, 115552.
23. X. Zhang, H. Su, P. Cui, Y. Cao, Z. Teng, Q. Zhang, Y. Wang, Y. Feng, R. Feng and J. Hou, *Nature Communications*, 2023, **14**, 7115.
24. X. Zhang, P. Ma, C. Wang, L. Gan, X. Chen, P. Zhang, Y. Wang, H. Li, L. Wang and X. Zhou, *Energy & Environmental Science*, 2022, **15**, 830-842.
25. Z. Wei, M. Liu, Z. Zhang, W. Yao, H. Tan and Y. Zhu, *Energy & Environmental Science*, 2018, **11**, 2581-2589.